

Research Article

Numerical Solution of the Modified Equal Width Wave Equation

Seydi Battal Gazi Karakoç and Turabi Geyikli

Department of Mathematics, Faculty of Education, İnönü University, 44280 Malatya, Turkey

Correspondence should be addressed to Seydi Battal Gazi Karakoç, sbgk44@mynet.com

Received 18 May 2011; Accepted 30 September 2011

Academic Editor: Sabri Arik

Copyright © 2012 S. B. G. Karakoç and T. Geyikli. This is an open access article distributed under the Creative Commons Attribution License, which permits unrestricted use, distribution, and reproduction in any medium, provided the original work is properly cited.

Numerical solution of the modified equal width wave equation is obtained by using lumped Galerkin method based on cubic B-spline finite element method. Solitary wave motion and interaction of two solitary waves are studied using the proposed method. Accuracy of the proposed method is discussed by computing the numerical conserved laws L_2 and L_∞ error norms. The numerical results are found in good agreement with exact solution. A linear stability analysis of the scheme is also investigated.

1. Introduction

The modified equal width wave equation (MEW) based upon the equal width wave (EW) equation [1, 2] which was suggested by Morrison et al. [3] is used as a model partial differential equation for the simulation of one-dimensional wave propagation in nonlinear media with dispersion processes. This equation is related with the modified regularized long wave (MRLW) equation [4] and modified Korteweg-de Vries (MKdV) equation [5]. All the modified equations are nonlinear wave equations with cubic nonlinearities and all of them have solitary wave solutions, which are wave packets or pulses. These waves propagate in non-linear media by keeping wave forms and velocity even after interaction occurs. Few analytical solutions of the MEW equation are known. Thus numerical solutions of the MEW equation can be important and comparison between analytic solution can be made. Geyikli and Battal Gazi Karakoç [6, 7] solved the MEW equation by a collocation method using septic B-spline finite elements and using a Petrov-Galerkin finite element method with weight functions quadratic and element shape functions which are cubic B-splines. Esen applied a lumped Galerkin method based on quadratic B-spline finite elements which have been used for solving the EW and MEW equation [8, 9]. Saka proposed algorithms for the numerical solution of the MEW equation using quintic B-spline collocation method [10].

Zaki considered the solitary wave interactions for the MEW equation by collocation method using quintic B-spline finite elements [11] and obtained the numerical solution of the EW equation by using least-squares method [12]. Wazwaz investigated the MEW equation and two of its variants by the tanh and the sine-cosine methods [13]. A solution based on a collocation method incorporated cubic B-splines is investigated by and Saka and Dağ [14]. Variational iteration method is introduced to solve the MEW equation by Lu [15]. Evans and Raslan [16] studied the generalized EW equation by using collocation method based on quadratic B-splines to obtain the numerical solutions of a single solitary waves and the birth of solitons. Hamdi et al. [17] derived exact solitary wave solutions of the generalized EW equation using Maple software. Esen and Kutluay studied a linearized implicit finite difference method in solving the MEW equation [18]. In the present work we solve the MEW equation numerically by a lumped Galerkin method using cubic B-spline finite elements. The accuracy of the proposed method is demonstrated by two test problems: the motion of a single solitary wave and the interaction of two solitary waves. A linear stability analysis based on a Fourier method shows that the numerical scheme is unconditionally stable.

2. Cubic B-Spline Lumped Galerkin Method

The modified equal width wave (MEW) equation considered here has the normalized form [3]

$$U_t + 3U^2U_x - \mu U_{xxt} = 0, \quad (2.1)$$

with the physical boundary conditions $U \rightarrow 0$ as $x \rightarrow \pm\infty$, where t is time, x is the space coordinate, μ is a positive parameter, and $U(x, t)$ is wave amplitude. In this study, boundary conditions are chosen from

$$\begin{aligned} U(a, t) = 0, \quad U(b, t) = 0, \\ U_x(a, t) = 0, \quad U_x(b, t) = 0, \quad t > 0, \end{aligned} \quad (2.2)$$

and the initial condition

$$U(x, 0) = f(x), \quad a \leq x \leq b, \quad (2.3)$$

where $f(x)$ is a localized disturbance inside interval $[a, b]$. The interval $[a, b]$ is partitioned into uniformly sized finite elements of length h by the knots x_m such that $a = x_0 < x_1 < \dots < x_N = b$ and $h = (x_{m+1} - x_m)$. The cubic B-splines $\phi_m(x)$, ($m = -1(1) N + 1$), at the knots x_m are defined over the interval $[a, b]$ by [19]

$$\phi_m(x) = \frac{1}{h^3} \begin{cases} (x - x_{m-2})^3, & x \in [x_{m-2}, x_{m-1}], \\ h^3 + 3h^2(x - x_{m-1}) + 3h(x - x_{m-1})^2 - 3(x - x_{m-1})^3, & x \in [x_{m-1}, x_m], \\ h^3 + 3h^2(x_{m+1} - x) + 3h(x_{m+1} - x)^2 - 3(x_{m+1} - x)^3, & x \in [x_m, x_{m+1}], \\ (x_{m+2} - x)^3, & x \in [x_{m+1}, x_{m+2}], \\ 0, & \text{otherwise.} \end{cases} \quad (2.4)$$

The set of functions $\{\phi_{-1}(x), \phi_0(x), \dots, \phi_{N+1}(x)\}$ forms a basis for functions defined over $[a, b]$. The approximate solution $U_N(x, t)$ to the exact solution $U(x, t)$ is given by

$$U_N(x, t) = \sum_{j=-1}^{N+1} \phi_j(x) \delta_j(t), \quad (2.5)$$

where δ_j are time-dependent parameters to be determined from the boundary and weighted residual conditions. Each cubic B-spline covers 4 elements so that each element $[x_m, x_{m+1}]$ is covered by 4 splines. In each element, using the following local coordinate transformation

$$h\xi = x - x_m, \quad 0 \leq \xi \leq 1, \quad (2.6)$$

cubic B-spline shape functions in terms of ξ over the element $[0, 1]$ can be defined as

$$\begin{aligned} \phi_{m-1} &= \begin{cases} (1 - \xi)^3, \\ 1 + 3(1 - \xi) + 3(1 - \xi)^2 - 3(1 - \xi)^3, \\ 1 + 3\xi + 3\xi^2 - 3\xi^3, \\ \xi^3. \end{cases} \\ \phi_m &= \\ \phi_{m+1} &= \\ \phi_{m+2} &= \end{aligned} \quad (2.7)$$

All splines apart from $\phi_{m-1}(x)$, $\phi_m(x)$, $\phi_{m+1}(x)$, and $\phi_{m+2}(x)$ are zero over the element $[0, 1]$. Variation of the function $U(x, t)$ over element $[0, 1]$ is approximated by

$$U_N(\xi, t) = \sum_{j=m-1}^{m+2} \delta_j \phi_j, \quad (2.8)$$

where $\delta_{m-1}, \delta_m, \delta_{m+1}, \delta_{m+2}$ act as element parameters and B-splines $\phi_{m-1}, \phi_m, \phi_{m+1}, \phi_{m+2}$ as element shape functions. Using trial function (2.5) and cubic splines (2.4), the values of U, U', U'' at the knots are determined in terms of the element parameters δ_m by

$$\begin{aligned} U_m &= U(x_m) = \delta_{m-1} + 4\delta_m + \delta_{m+1}, \\ U'_m &= U'(x_m) = 3(-\delta_{m-1} + \delta_{m+1}), \\ U''_m &= U''(x_m) = 6(\delta_{m-1} - 2\delta_m + \delta_{m+1}), \end{aligned} \quad (2.9)$$

where the symbols ' and '' denote first and second differentiation with respect to x , respectively. The splines $\phi_m(x)$ and its two principle derivatives vanish outside the interval $[x_{m-2}, x_{m+2}]$. Use Galerkin's method with weight function $W(x)$ to obtain the weak form of (2.1) which is

$$\int_a^b W(U_t + 3U^2 U_x - \mu U_{xxt}) dx = 0. \quad (2.10)$$

For a single element $[x_m, x_{m+1}]$ using transformation (2.6) into the (2.10) we obtain

$$\int_0^1 W \left(U_t + \frac{3}{h} \widehat{U}^2 U_\xi - \frac{\mu}{h^2} U_{\xi\xi t} \right) d\xi = 0, \quad (2.11)$$

where \widehat{U} is taken to be a constant over an element to simplify the integral. Integrating (2.11) by parts leads to

$$\int_0^1 [WU_t + \lambda WU_\xi + \beta W_\xi U_{\xi t}] d\xi = \beta WU_{\xi t} \Big|_0^1 \quad (2.12)$$

where $\lambda = 3\widehat{U}^2/h$ and $\beta = \mu/h^2$. Taking the weight function with cubic B-spline shape functions given by (2.7) and substituting approximation (2.8) in integral equation (2.12) with some manipulation, we obtain the element contributions in the form

$$\sum_{j=m-1}^{m+2} \left[\left(\int_0^1 \phi_i \phi_j + \beta \phi_i' \phi_j' \right) d\xi - \beta \phi_i \phi_j' \Big|_0^1 \right] \delta_j^e + \sum_{j=m-1}^{m+2} \left(\lambda \int_0^1 \phi_i \phi_j' d\xi \right) \delta_j^e. \quad (2.13)$$

In matrix notation this equation becomes

$$[A^e + \beta(B^e - C^e)] \delta^e + \lambda D^e \delta^e, \quad (2.14)$$

where $\delta^e = (\delta_{m-1}, \delta_m, \delta_{m+1}, \delta_{m+2})^T$ are the element parameters and the dot denotes differentiation with respect to t . The element matrices A^e, B^e, C^e , and D^e are given by the following integrals:

$$A_{ij}^e = \int_0^1 \phi_i \phi_j d\xi = \frac{1}{140} \begin{bmatrix} 20 & 129 & 60 & 1 \\ 129 & 1188 & 933 & 60 \\ 60 & 933 & 1188 & 129 \\ 1 & 60 & 129 & 20 \end{bmatrix},$$

$$B_{ij}^e = \int_0^1 \phi_i' \phi_j' d\xi = \frac{1}{10} \begin{bmatrix} 18 & 21 & -36 & -3 \\ 21 & 102 & -87 & -36 \\ -36 & -87 & 102 & 12 \\ -3 & -36 & 21 & 18 \end{bmatrix},$$

$$C_{ij}^e = \phi_i \phi_j' \Big|_0^1 = 3 \begin{bmatrix} 1 & 0 & -1 & 0 \\ 4 & -1 & -4 & 1 \\ 1 & -4 & -1 & 4 \\ 0 & -1 & 0 & 1 \end{bmatrix},$$

$$D_{ij}^e = \int_0^1 \phi_i \phi_j' d\xi = \frac{1}{20} \begin{bmatrix} -10 & -9 & 18 & 1 \\ -71 & -150 & 183 & 38 \\ -38 & -183 & 150 & 71 \\ -1 & -18 & 9 & 10 \end{bmatrix},$$
(2.15)

where the suffices i, j take only the values $m-1, m, m+1, m+2$ for the typical element $[x_m, x_{m+1}]$. A lumped value for λ is found from $(1/4)(U_m + U_{m+1})^2$ as

$$\lambda = \frac{3}{4h} (\delta_{m-1} + 5\delta_m + 5\delta_{m+1} + \delta_{m+2})^2. \quad (2.16)$$

By assembling all contributions from all elements, (2.14) leads to the following matrix equation:

$$[A^e + \beta(B^e - C^e)]\delta^e + \lambda D^e \delta^e = 0, \quad (2.17)$$

where $\delta = (\delta_{-1}, \delta_0 \cdots \delta_N, \delta_{N+1})^T$ is a global element parameter. The matrices A, B , and λD are septadiagonal and row of each has the following form:

$$A = \frac{1}{140} (1, 120, 1191, 2416, 1191, 120, 1),$$

$$B = \frac{1}{10} (-3, -72, -45, 240, -45, -72, -3),$$

$$\lambda D = \frac{1}{20} (-\lambda_1, -18\lambda_1 - 38\lambda_2, 9\lambda_1 - 183\lambda_2 - 71\lambda_3, 10\lambda_1 + 150\lambda_2 - 150\lambda_3 - 10\lambda_4, \\ 71\lambda_2 + 183\lambda_3 - 9\lambda_4, 38\lambda_3 + 18\lambda_4, \lambda_4),$$
(2.18)

where

$$\lambda_1 = \frac{3}{4h} (\delta_{m-2} + 5\delta_{m-1} + 5\delta_m + \delta_{m+1})^2,$$

$$\lambda_2 = \frac{3}{4h} (\delta_{m-1} + 5\delta_m + 5\delta_{m+1} + \delta_{m+2})^2,$$

$$\lambda_3 = \frac{3}{4h} (\delta_m + 5\delta_{m+1} + 5\delta_{m+2} + \delta_{m+3})^2,$$

$$\lambda_4 = \frac{3}{4h} (\delta_{m+1} + 5\delta_{m+2} + 5\delta_{m+3} + \delta_{m+4})^2.$$
(2.19)

Replacing the time derivative of the parameter $\dot{\delta}$ by usual forward finite difference approximation and parameter δ by the Crank-Nicolson formulation

$$\dot{\delta} = \frac{\delta^{n+1} - \delta^n}{\Delta t}, \quad \delta = \frac{1}{2}(\delta^n + \delta^{n+1}) \quad (2.20)$$

into equation (2.17), gives the $(N + 3) \times (N + 3)$ septadiagonal matrix system

$$\left[A + \beta(B - C) + \frac{\lambda \Delta t}{2} D \right] \delta^{n+1} = \left[A + \beta(B - C) - \frac{\lambda \Delta t}{2} D \right] \delta^n, \quad (2.21)$$

where Δt is time step. Applying the boundary conditions (2.2) to the system (2.21) we obtain an $(N + 1) \times (N + 1)$ septadiagonal matrix system. This system is efficiently solved with a variant of the Thomas algorithm, but an inner iteration is also needed at each time step to cope with the non-linear term. A typical member of the matrix system (2.21) may be written in terms of the nodal parameters δ^n and δ^{n+1} as

$$\begin{aligned} & \gamma_1 \delta_{m-2}^{n+1} + \gamma_2 \delta_{m-1}^{n+1} + \gamma_3 \delta_m^{n+1} + \gamma_4 \delta_{m+1}^{n+1} + \gamma_5 \delta_{m+2}^{n+1} + \gamma_6 \delta_{m+3}^{n+1} + \gamma_7 \delta_{m+4}^{n+1} \\ & = \gamma_7 \delta_{m-2}^n + \gamma_6 \delta_{m-1}^n + \gamma_5 \delta_m^n + \gamma_4 \delta_{m+1}^n + \gamma_3 \delta_{m+2}^n + \gamma_2 \delta_{m+3}^n + \gamma_1 \delta_{m+4}^n, \end{aligned} \quad (2.22)$$

where

$$\begin{aligned} \gamma_1 &= \frac{1}{140} - \frac{3\beta}{10} - \frac{\lambda \Delta t}{40}, \\ \gamma_2 &= \frac{120}{140} - \frac{72\beta}{10} - \frac{56\lambda \Delta t}{40}, \\ \gamma_3 &= \frac{1191}{140} - \frac{45\beta}{10} - \frac{245\lambda \Delta t}{40}, \\ \gamma_4 &= \frac{2416}{140} + \frac{240\beta}{10}, \\ \gamma_5 &= \frac{1191}{140} - \frac{45\beta}{10} + \frac{245\lambda \Delta t}{40}, \\ \gamma_6 &= \frac{120}{140} - \frac{72\beta}{10} + \frac{56\lambda \Delta t}{40}, \\ \gamma_7 &= \frac{1}{140} - \frac{3\beta}{10} + \frac{\lambda \Delta t}{40} \end{aligned} \quad (2.23)$$

which all depend on δ^n . The initial vector of parameter $\delta^0 = (\delta_{-1}^0, \dots, \delta_{N+1}^0)$ must be determined to iterate system (2.21). To do this, the approximation is rewritten over the interval $[a, b]$ at time $t = 0$ as follows:

$$U_N(x, 0) = \sum_{m=-1}^{N+1} \phi_m(x) \delta_m^0, \quad (2.24)$$

where the parameters δ_m^0 will be determined. $U_N(x, 0)$ are required to satisfy the following relations at the mesh points x_m :

$$\begin{aligned} U_N(x_m, 0) &= U(x_m, 0), \quad m = 0, 1, \dots, N, \\ U'_N(x_0, 0) &= U'(x_N, 0) = 0. \end{aligned} \quad (2.25)$$

The above conditions lead to a tridiagonal matrix system of the form

$$\begin{bmatrix} -3 & 0 & 3 & & & \\ 1 & 4 & 1 & & & \\ & & \ddots & & & \\ & & & 1 & 4 & 1 \\ & & & & -3 & 0 & 3 \end{bmatrix} \begin{bmatrix} \delta_{-1}^0 \\ \delta_0^0 \\ \vdots \\ \delta_N^0 \\ \delta_{N+1}^0 \end{bmatrix} = \begin{bmatrix} 0 \\ U(x_0) \\ \vdots \\ U(x_N) \\ 0 \end{bmatrix} \quad (2.26)$$

which can be solved using a variant of the Thomas algorithm.

2.1. Stability Analysis

The stability analysis is based on the Von Neumann theory in which the growth factor g of the error in a typical mode of amplitude $\hat{\delta}^n$,

$$\delta_j^n = \hat{\delta}^n e^{ijkh}, \quad (2.27)$$

where k is the mode number and h the element size, is determined from a linearization of the numerical scheme. To apply the stability analysis, the MEW equation needs to be linearized by assuming that the quantity U in the non-linear term $U^2 U_x$ is locally constant. Substituting the Fourier mode (2.27) into (2.22) gives the growth factor g of the form

$$g = \frac{a - ib}{a + ib}, \quad (2.28)$$

where

$$\begin{aligned} a &= 2416 + 3360\beta + (2382 - 1260\beta) \cos \theta h + (240 - 2016\beta) \cos 2\theta h + (2 - 84\beta) \cos 3\theta h, \\ b &= 5145\lambda \Delta t \sin \theta h + 1176\lambda \Delta t \sin 2\theta h + 21\lambda \Delta t \sin 3\theta h. \end{aligned} \quad (2.29)$$

The modulus of $|g|$ is 1, therefore the linearized scheme is unconditionally stable.

3. Numerical Examples and Results

In this part, we consider the following two test problems: the motion of a single solitary wave and interaction of two solitary waves. All computations are executed on a Pentium 4 PC in

the Fortran code using double precision arithmetic. For the MEW equation, it is important to discuss the following three invariant conditions given in [11], which, respectively, correspond to conservation of mass, momentum, and energy. The accuracy of the method is measured by both the L_2 error norm

$$\begin{aligned} C_1 &= \int_a^b U \, dx \simeq h \sum_{j=1}^N U_j^n, \\ C_2 &= \int_a^b U^2 + \mu(U_x)^2 \, dx \simeq h \sum_{j=1}^N (U_j^n)^2 + \mu(U_x)_j^n, \\ C_3 &= \int_a^b U^4 \, dx \simeq h \sum_{j=1}^N (U_j^n)^4, \end{aligned} \quad (3.1)$$

$$L_2 = \|U^{\text{exact}} - U_N\|_2 \simeq \sqrt{h \sum_{j=0}^N |U_j^{\text{exact}} - (U_N)_j|^2} \quad (3.2)$$

and the L_∞ error norm

$$L_\infty = \|U^{\text{exact}} - U_N\|_\infty \simeq \max_j |U_j^{\text{exact}} - (U_N)_j| \quad (3.3)$$

to show how well the scheme predicts the position and amplitude of the solution as the simulation proceeds. The variable U_j^n and its first derivative appearing in (3.1) can be computed from (2.9), respectively.

3.1. The Motion of Single Solitary Wave

For this problem we consider (2.1) with the boundary condition $U \rightarrow 0$ as $x \rightarrow \pm\infty$ and the initial condition

$$U(x, 0) = A \operatorname{sech}[k(x - x_0)]. \quad (3.4)$$

An exact solution of this problem is given by [11]

$$U(x, t) = A \operatorname{sech}[k(x - x_0 - vt)] \quad (3.5)$$

which represents the motion of a single solitary wave with amplitude A , where the wave velocity $v = A^2/2$ and $k = \sqrt{1/\mu}$. For this problem the analytical values of the invariants are [11]

$$C_1 = \frac{A\pi}{k}, \quad C_2 = \frac{2A^2}{k} + \frac{2\mu k A^2}{3}, \quad C_3 = \frac{4A^4}{3k}. \quad (3.6)$$

Table 1: Invariants and error norms for single solitary wave with $h = 0.1, \Delta t = 0.05$.

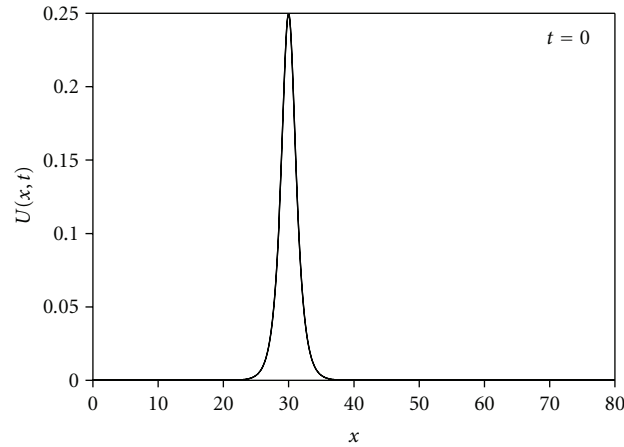
t	C_1	C_2	C_3	$L_2 \times 10^3$	$L_\infty \times 10^3$
0	0.7853966	0.1666661	0.0052083	0.0000000	0.0000000
5	0.7853966	0.1666662	0.0052083	0.0204838	0.0115451
10	0.7853966	0.1666662	0.0052083	0.0407743	0.0231561
15	0.7853967	0.1666662	0.0052083	0.0606975	0.0347169
20	0.7853967	0.1666663	0.0052083	0.0800980	0.0460618
20 [9]	0.7853898	0.1667614	0.0052082	0.0796940	0.0465523
20 [16]	0.7849545	0.1664765	0.0051995	0.2905166	0.2498925
20 [18]	0.7853977	0.1664735	0.0052083	0.2692812	0.2569972

For the numerical simulation of the motion of a single solitary wave, we choose the parameters $h = 0.1, \Delta t = 0.05, \mu = 1, x_0 = 30, A = 0.25$ through the interval $0 \leq x \leq 80$. The analytical values for the invariants are $C_1 = 0.7853982, C_2 = 0.1666667, C_3 = 0.0052083$. The invariants C_1 and C_2 change from their initial values by less than 1×10^{-7} and 2×10^{-7} respectively, during the time of running, whereas the changes of invariant C_3 approach to zero throughout. The computations are done until time $t = 20$, and we find L_2, L_∞ error norms and numerical invariants C_1, C_2, C_3 at various times. Results are documented in Table 1. One may also compare our results with those in the other studies [9, 16, 18]. According to both L_2, L_∞ error norms, agreement between numerical values and exact solution appears very satisfactorily through illustrations of three invariants and norms. Figure 1 shows that the proposed method performs the motion of propagation of a solitary wave satisfactorily, which moved to the right at a constant speed and preserved its amplitude and shape with increasing time as expected. Amplitude is 0.25 at $t = 0$ which is located at $x = 30$, while it is 0.249900 at $t = 20$ which is located at $x = 30.6$. The absolute difference in amplitudes at times $t = 0$ and $t = 20$ is 1×10^{-4} so that there is a little change between amplitudes. The convergence rates for the numerical method in space sizes h_m and time steps $U_{\Delta t_m}$ can be calculated by following formula [9], respectively,

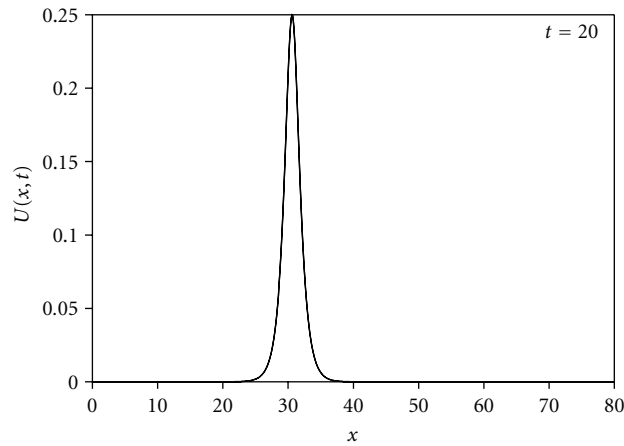
$$\text{order} = \frac{\log_{10}\left(\left|U^{\text{exact}} - U_{h_m}^{\text{num}}\right| / \left|U^{\text{exact}} - U_{h_{m+1}}^{\text{num}}\right|\right)}{\log_{10}(h_m/h_{m+1})}, \tag{3.7}$$

$$\text{order} = \frac{\log_{10}\left(\left|U^{\text{exact}} - U_{\Delta t_m}^{\text{num}}\right| / \left|U^{\text{exact}} - U_{\Delta t_{m+1}}^{\text{num}}\right|\right)}{\log_{10}(\Delta t_m/\Delta t_{m+1})}.$$

Table 2 displays the convergence rates for different values of space size h and a fixed value of the time step Δt_m . We have clearly seen that the convergence rates when Δt is fixed are not good these for size. In addition, the time rate of the convergence for the numerical method is computed with various time step $U_{\Delta t_m}$ and fixed space step h in Table 3. It can clearly be seen that the present method provides remarkable reductions in convergence rates for the smaller time.



(a)



(b)

Figure 1: The motion of a single solitary wave with $h = 1$, $\Delta t = 0.05$ at $t = 0$ and $t = 20$.

3.2. Interaction of Two Solitary Waves

In this section, we consider (2.1) with boundary conditions $U \rightarrow 0$ as $x \rightarrow \pm\infty$ and the initial condition

$$U(x,0) = \sum_{j=1}^2 A_j \operatorname{sech}(k[x - x_j]) \quad (3.8)$$

where $k = \sqrt{1/\mu}$.

Firstly we studied the interaction of two positive solitary waves with the parameters $h = 0.1$, $\Delta t = 0.025$, $\mu = 1$, $A_1 = 1$, $A_2 = 0.5$, $x_1 = 15$, $x_2 = 30$ through the interval $0 \leq x \leq 80$ which used the earlier papers [9–11]. The analytic invariants are [16] $C_1 = \pi(A_1 + A_2) = 4.7123889$, $C_2 = (8/3)(A_1^2 + A_2^2) = 3.3333333$, $C_3 = (4/3)(A_1^4 + A_2^4) = 1.4166667$ and changes in C_1, C_2 , and C_3 are less than 4.1×10^{-3} , 4.3×10^{-3} , and 3.6×10^{-3} percent, respectively, as

Table 2: The order of convergence at $t = 20, \Delta t = 0.05, A = 0.25$.

h_m	$L_2 \times 10^3$	order	$L_\infty \times 10^3$	order
0.8	4.16296467	—	2.78665608	—
0.4	1.21228931	1.77987727	0.68462204	2.02515531
0.2	0.31752640	1.93278558	0.18175645	1.91330117
0.1	0.08009801	1.9803824	0.04606181	1.98036355
0.05	0.01932448	2.05133680	0.01122974	2.03624657
0.025	0.00530959	1.86375722	0.00304044	1.88497250

Table 3: The order of convergence at $t = 20, h = 0.1, A = 0.25$.

Δt_m	$L_2 \times 10^3$	order	$L_\infty \times 10^3$	order
0.8	0.08383192	—	0.08300304	—
0.4	0.07424489	0.17520793	0.05061152	0.71369837
0.2	0.07833790	-0.07817543	0.04448503	0.18614587
0.1	0.07972878	-0.02539013	0.04573242	-0.03989733
0.05	0.08009801	-0.00666580	0.04606181	-0.01035383
0.025	0.08019167	-0.00168598	0.04614408	-0.00257446

Table 4: Invariants for the interaction of two solitary waves.

t	$A_1 = 1, A_2 = 0.5 (0 \leq x \leq 80)$			$A_1 = -2, A_2 = 1 (0 \leq x \leq 150)$		
	C_1	C_2	C_3	C_1	C_2	C_3
0	4.7123732	3.3333253	1.4166643	-3.1415737	13.3332816	22.6665313
5	4.7123861	3.3333482	1.4166852	-3.1458603	13.3449843	22.7133525
10	4.7123959	3.3333621	1.4166982	-3.1377543	13.3031153	22.5832812
15	4.7124065	3.3333785	1.4167141	-3.1625436	13.3838991	22.8926223
20	4.7124249	3.3334164	1.4167521	-3.1658318	13.3999304	22.9451481
25	4.7124899	3.3335832	1.4169238	-3.1701819	13.4126391	22.9954601
30	4.7127643	3.3333557	1.4177617	-3.1747553	13.4251358	22.0458834
35	4.7130474	3.3352500	1.4188849	-3.1793707	13.4376785	23.0966349
40	4.7124881	3.3336316	1.4171690	-3.1840126	13.4502895	23.1477374
45	4.7123002	3.3331878	1.4167580	-3.1886789	13.4629730	23.1991979
50	4.7122479	3.3330923	1.4167142	-3.1933699	13.4757303	23.2510209
55	4.7122576	3.3331149	1.4167237	-3.1980856	13.4885624	23.3032108

can be seen in Table 4. The experiment was run from $t = 0$ to $t = 55$ to allow the interaction to take place. This condition is propagated to the right with velocities dependent upon their magnitudes and a stage is reached where the larger wave has passed through the smaller solitary wave and has emerged with their original shapes. Figure 2 shows the interactions of two positive solitary waves. Interaction started at about time $t = 25$, overlapping processes occurred between times $t = 25$ and $t = 40$ and, waves started to resume their original shapes after time $t = 40$. It can be seen that, at $t = 5$, the wave with larger amplitude is on the left of the second wave with smaller amplitude. The larger wave catches up with the smaller one as time increases. At $t = 55$, the amplitude of larger waves is 0.999581 at the point $x = 44.4$ whereas the amplitude of the smaller one is 0.510464 at the point $x = 34.7$. It is found that the absolute difference in amplitude is 1.04×10^{-1} for the smaller wave and 0.419×10^{-3} for

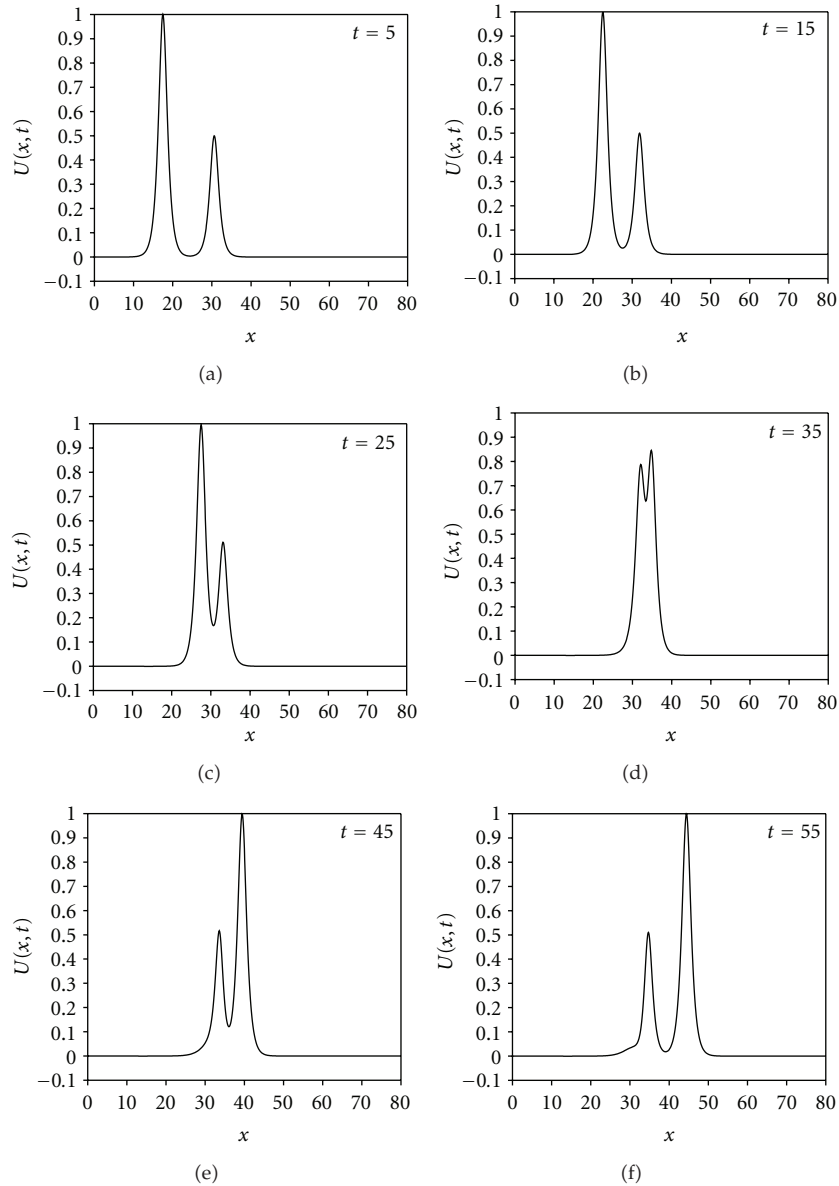


Figure 2: Interaction of two solitary waves at different times.

the larger wave for this algorithm. Finally, we have studied the interaction of two solitary waves with the following parameters, $\mu = 1$, $x_1 = 15$, $x_2 = 30$, $A_1 = -2$, $A_2 = 1$ together with time step $\Delta t = 0.025$ and space step $h = 0.1$ in the range $0 \leq x \leq 150$. The experiment was run from $t = 0$ to $t = 55$ to allow the interaction to take place. Figure 3 shows the development of the solitary wave interaction. As is seen from Figure 3, at $t = 0$, a wave with the negative amplitude is on the left of another wave with the positive amplitude. The larger wave with the negative amplitude catches up with the smaller one with the positive amplitude as the time increases. At $t = 55$, the amplitude of the smaller wave is 0.972910 at the point

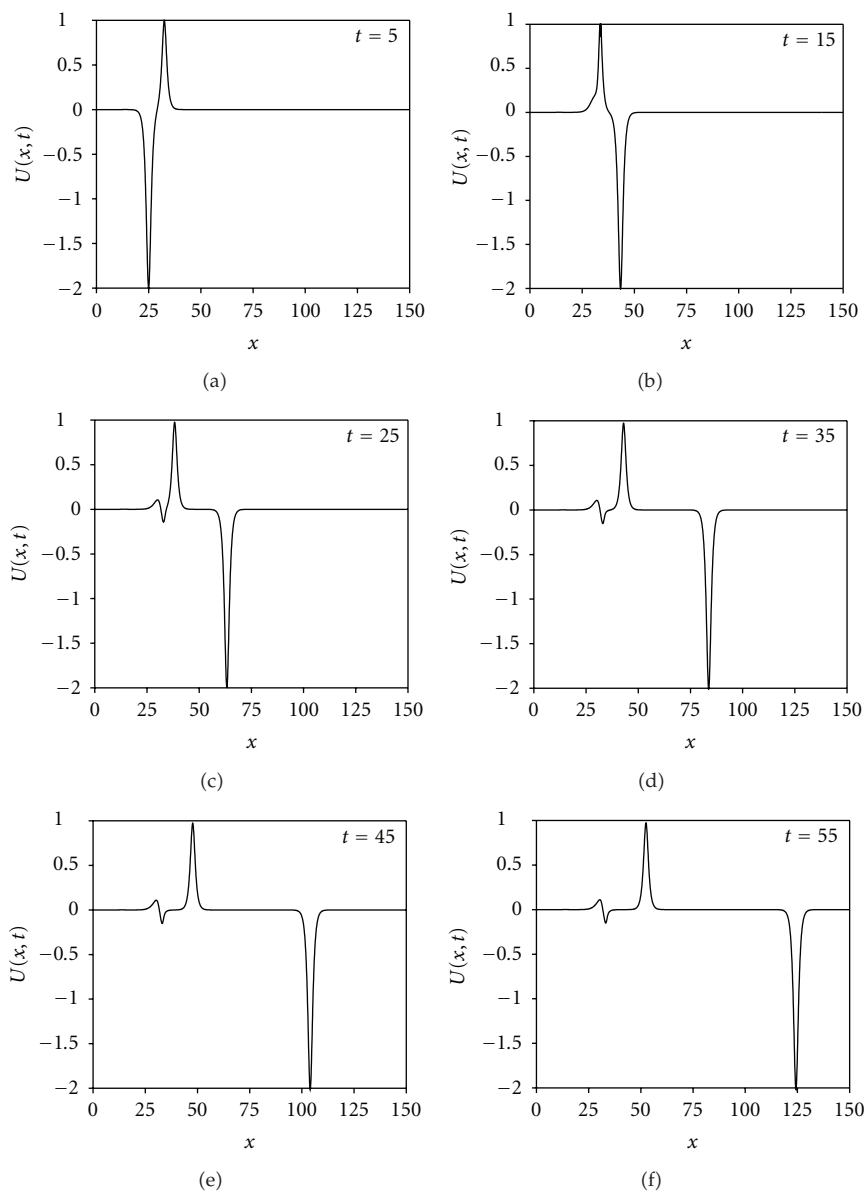


Figure 3: Interaction of two solitary waves at different times.

$x = 52.5$, whereas the amplitude of the larger one is -2.016990 at the point $x = 124.3$. It is found that the absolute difference in amplitudes is 0.27×10^{-1} for the smaller wave and 0.16×10^{-1} for the larger wave. The analytical invariants can be found as $C_1 = -3.1415927$, $C_2 = 13.3333333$, $C_3 = 22.6666667$ and changes in C_1 , C_2 , and C_3 are less than 10.5×10^{-3} , 3.7×10^{-3} , and 10.9×10^{-3} , percent, respectively. Table 4 lists the values of the invariants of the two solitary waves with amplitudes $A_1 = 1$, $A_2 = 0.5$, and $A_1 = -2$, $A_2 = 1$. It can be seen that the values obtained for the invariants are satisfactorily constant during the computer run. We have also compared the computed values of the invariants of the two solitary waves with results from [9] in Table 5.

Table 5: Comparison of invariants for the interaction of two solitary waves with results from [9] with $h = 0.1$, $\Delta t = 0.025$, $A_1 = 1$, $A_2 = 0.5$, ($0 \leq x \leq 80$).

t	C_1	C_2	C_3	C_1 [9]	C_2 [9]	C_3 [9]
0	4.7123732	3.3333253	1.4166643	4.7123884	3.3352890	1.4166697
5	4.7123861	3.3333482	1.4166852	4.7123718	3.3352635	1.4166486
10	4.7123959	3.3333621	1.4166982	4.7123853	3.3352836	1.4166647
15	4.7124065	3.3333785	1.4167141	4.7123756	3.3352894	1.4166772
20	4.7124249	3.3334164	1.4167521	4.7123748	3.3353041	1.4166926
25	4.7124899	3.3335832	1.4169238	4.7124173	3.3354278	1.4168363
30	4.7127643	3.3333557	1.4177617	4.7126410	3.3359464	1.4176398
35	4.7130474	3.3352500	1.4188849	4.7128353	3.3364247	1.4186746
40	4.7124881	3.3336316	1.4171690	4.7123946	3.3355951	1.4170695
45	4.7123002	3.3331878	1.4167580	4.7122273	3.3352364	1.4166637
50	4.7122479	3.3330923	1.4167142	4.7121567	3.3351175	1.4165797
55	4.7122576	3.3331149	1.4167237	4.7121400	3.3350847	1.4165527

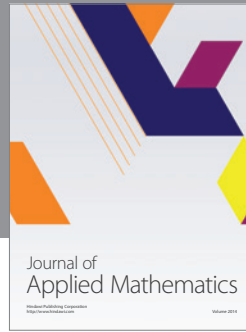
4. Conclusion

In this paper, the cubic B-spline lumped Galerkin method has been successfully applied to obtain the numerical solution of the modified equal width wave equation. The efficiency of the method was tested on two test problems of wave propagation: the motion of a single solitary wave and the interaction of two solitary waves, and its accuracy was shown by calculating error norms L_2 and L_∞ . It is clear that the error norms are adequately small and the invariants are satisfactorily constant in all computer run. The method can be also efficiently applied for solving a large number of physically important non-linear problems.

References

- [1] L. R. T. Gardner and G. A. Gardner, "Solitary waves of the regularised long-wave equation," *Journal of Computational Physics*, vol. 91, no. 2, pp. 441–459, 1990.
- [2] L. R. T. Gardner and G. A. Gardner, "Solitary waves of the equal width wave equation," *Journal of Computational Physics*, vol. 101, no. 1, pp. 218–223, 1992.
- [3] P. J. Morrison, J. D. Meiss, and J. R. Cary, "Scattering of regularized-long-wave solitary waves," *Physica D. Nonlinear Phenomena*, vol. 11, no. 3, pp. 324–336, 1984.
- [4] Kh. O. Abdulloev, I. L. Bogolubsky, and V. G. Makhankov, "One more example of inelastic soliton interaction," *Physics Letters. A*, vol. 56, no. 6, pp. 427–428, 1976.
- [5] L. R. T. Gardner, G. A. Gardner, and T. Geyikli, "The boundary forced MKdV equation," *Journal of Computational Physics*, vol. 113, no. 1, pp. 5–12, 1994.
- [6] T. Geyikli and S. Battal Gazi Karakoç, "Septic B-Spline Collocation Method for the Numerical Solution of the Modified Equal Width Wave Equation," *Applied Mathematics*, vol. 2, no. 6, pp. 739–749, 2011.
- [7] T. Geyikli and S. Battal Gazi Karakoç, "Petrov-Galerkin method with cubic Bsplines for solving the MEW equation," *Bulletin of the Belgian Mathematical Society*. In press.
- [8] A. Esen, "A numerical solution of the equal width wave equation by a lumped Galerkin method," *Applied Mathematics and Computation*, vol. 168, no. 1, pp. 270–282, 2005.
- [9] A. Esen, "A lumped Galerkin method for the numerical solution of the modified equal-width wave equation using quadratic B-splines," *International Journal of Computer Mathematics*, vol. 83, no. 5-6, pp. 449–459, 2006.
- [10] B. Saka, "Algorithms for numerical solution of the modified equal width wave equation using collocation method," *Mathematical and Computer Modelling*, vol. 45, no. 9-10, pp. 1096–1117, 2007.
- [11] S. I. Zaki, "Solitary wave interactions for the modified equal width equation," *Computer Physics Communications*, vol. 126, no. 3, pp. 219–231, 2000.

- [12] S. I. Zaki, "Least-squares finite element scheme for the EW equation," *Computer Methods in Applied Mechanics and Engineering*, vol. 189, no. 2, pp. 587–594, 2000.
- [13] A.-M. Wazwaz, "The tanh and the sine-cosine methods for a reliable treatment of the modified equal width equation and its variants," *Communications in Nonlinear Science and Numerical Simulation*, vol. 11, no. 2, pp. 148–160, 2006.
- [14] B. Saka and Dağ, "Quartic B-spline collocation method to the numerical solutions of the Burgers' equation," *Chaos, Solitons and Fractals*, vol. 32, no. 3, pp. 1125–1137, 2007.
- [15] J. Lu, "He's variational iteration method for the modified equal width equation," *Chaos, Solitons and Fractals*, vol. 39, no. 5, pp. 2102–2109, 2009.
- [16] D. J. Evans and K. R. Raslan, "Solitary waves for the generalized equal width (GEW) equation," *International Journal of Computer Mathematics*, vol. 82, no. 4, pp. 445–455, 2005.
- [17] S. Hamdi, W. H. Enright, W. E. Schiesser, and J. J. Gottlieb, "Exact solutions of the generalized equal width wave equation," in *Proceedings of the International Conference on Computational Science and Its Application*, vol. 2668, pp. 725–734, Springer, 2003.
- [18] A. Esen and S. Kutluay, "Solitary wave solutions of the modified equal width wave equation," *Communications in Nonlinear Science and Numerical Simulation*, vol. 13, no. 8, pp. 1538–1546, 2008.
- [19] P. M. Prenter, *Splines and Variational Methods*, John Wiley & Sons, New York, NY, USA, 1975.



Hindawi

Submit your manuscripts at
<http://www.hindawi.com>

